DMD Fast Forward. Published on September 9, 2009 as doi:10.1124/dmd.109.029520

DMD 29520

PURIFICATION AND MECHANISM OF HUMAN ALDEHYDE OXIDASE (AOX1) EXPRESSED IN E. COLI.*

Joshua F. Alfaro, Carolyn A. Joswig-Jones, Wenyun Ouyang, Joseph Nichols, Gregory J. Crouch and Jeffrey P. Jones.

Department of Chemistry, Washington State University, Pullman WA 99163

Running title Page

EXPRESSION OF HUMAN ALDEHYDE OXIDASE

Address correspondence to: Jeffrey. P. Jones, Department of Chemistry, Washington State University, Pullman WA 99163. Phone: 505-335-5983, Fax: 509-335-8867, E-mail: jpj@wsu.edu

number of text pages:

number of tables: 2

number of figures: 3

number of references: 38

number of words in the Abstract: 121

number of words in the Introduction: 693

number of words in the Discussion:

The abbreviations used are:

AOX1, Aldehyde Oxidase 1

XO, Xanthine Oxidase

PCR, polymerase chain reaction

KIE, Kinetic isotope effect

DMD Fast Forward. Published on September 9, 2009 as DOI: 10.1124/dmd.109.029520
This article has not been copyedited and formatted. The final version may differ from this version.

Abstract

Human aldehyde oxidase 1 (AOX1) has been subcloned into a vector suitable for expression in E. coli and the protein expressed. The resulting protein is active, with sulfur being incorporated in the molybdopterin cofactor. Expression levels are modest, but one liter of cells supplies enough protein for both biochemical and kinetic characterization. Partial purification is achieved by nickel affinity chromatography through the addition of 6 histidines to the amino terminal end of the protein. Kinetic analysis, including kinetic isotope effects and comparison with xanthine oxidase, reveal similar mechanisms, with some subtle differences. This expression system will allow for the interrogation of human aldehyde oxidase structure/function relationships by site-directed mutagenesis, and provides protein for characterizing the role of AOX1 in drug metabolism.

Introduction

Over the past decade there has been a growing awareness that metabolism can play a major role in drug development and toxicity (O'Brien and de Groot 2005; Rettie and Jones 2005). In particular, drug design has evolved in the direction of more metabolically stable molecules, often with the major metabolite being oxidation of an aromatic ring by cytochrome P450 enzymes. This leads to reasonable pharmacokinetics, however the oxidation products can show toxicity. One method to slow aromatic oxidation is incorporation of a nitrogen to make a hetereoaromatic ring (Dowers et al. 2004). The electron withdrawing characteristics of nitrogen slow the electrophilic chemistry of the P450 enzymes. The net result can lead to a change in the metabolic pathways to nucleophilic addition by the molybdenum iron-sulfur flavoproteins, xanthine oxidase (XO) and aldehyde oxidase (AOX) (Obach and Walsky 2005). Both XO and AO can oxidize aldehydes and nitrogen containing aromatic compounds (Figure 1) (Beedham et al. 1990; Panoutsopoulos and Beedham 2004). At present over 40 drugs, nutritional supplements, and xenobiotics are metabolized to some extent by AOX (Kitamura et al. 2006). Given that the changes in structural characteristics to decrease P450 metabolism have only been happening over the past 10 years we should see a significant increase in the importance of XO and AOX in drug metabolism over the next decade as these drug design efforts result in drugs (Obach et al. 2004).

XO has a reasonably well defined physiological role in the metabolism of purines (Garattini et al. 2008), while the physiological role of AOX is only recently being defined in mammals. The role of these enzymes in plants has received more attention (Mendel 2007). Knock-down experiments on AOX1 (the mouse ortholog of the only active human enzyme) in mice indicate that this enzyme plays a functional role in adipogenesis (Weigert et al. 2008). While knockout of AOH2 in mice show a decrease in retinoid-dependent genes, and alteration of the epidermis (Terao et al. 2009).

One confounding feature in both drug metabolism and in understanding the physiological roles of AOX enzymes is that significant interspecies variations exist in both the number and activity of mammalian enzymes. For example, the major species used in early drug development (mice, rats and dogs) have a number of AOX enzymes while humans only have a single AOX enzyme. Dogs in general have low activity, and two active AOX enzymes, whereas rats and mice have four enzymes and show a marked interspecies variation in metabolism, while humans have a single highly active AOX (AOX1) (Kitamura et al. 2006; Terao et al. 2006; Garattini et al. 2008). These interspecies differences mean that standard animal models will underestimate clearance, potentially leading to ineffective drugs due to rapid clearance when the compounds enter clinical trials. Human AOX1 has been partially purified from human liver and substrate specificity assessed and compared to guinea pig, rabbit, and baboon (Beedham et al. 1995).

Another interesting feature of AOX is that the end electron acceptor is oxygen resulting in the production of reactive oxygen species. These reactive oxygen species have been implicated in Amyotrophic Lateral Sclerosis (ALS), otherwise known as "Lou Gehrig's Disease," (Berger et al. 1995) and in ethanol induced liver injury (Moriwaki et al. 1997). Presently it is unknown if increasing turnover of AOX would lead to pathology as a result of increased reactive oxygen species. Another concern is that drugs that are substrates for AOX1 will alter adipose tissue homeostasis (Weigert et al. 2008).

Currently, if drugs are even screened, the major tool used in early drug discovery to identify the role of XO or AOX1 is human liver cytosol (Obach et al. 2004). Since both XO and AOX metabolize similar substrates, inhibitors specific for each enzyme are used to determine which enzyme plays the major role in metabolism (Rashidi et al. 1997). While the expression of human XO in E. coli has been reported (Yamaguchi et al. 2007), to our knowledge no expression system is available for human AO. To this end we have expressed and partially purified human AO in E. coli. Partial purification is done by incorporation of 6 histidines onto the amino terminus followed by affinity chromatography. Mechanistic

comparisons using substituent effects and kinetic isotope effects with bovine XO, confirm the speculation that AO and XO have a relatively similar chemical and kinetic mechanisms.

Methods

Materials- All reagents were purchased from Sigma Aldrich at reagent grade purity or finer unless specified otherwise. Anthranilic acid was from J.T. Baker Chemical Co., 2-amino-5-nitrobenzoic acid was from Alfa Aesar (Ward Hill, MA).

Construction of expression vector- The vector was constructed using a similar strategy as described by Tanaka and coworkers (Hoshino et al. 2007). The protein coding region of human aldehyde oxidase cDNA in a pCMV6-XL4 mammalian plasmid was PCR-amplified using PfuUltra Hotstart PCR Master Mix (Stratagene). The primers used for amplification were 5'-TAC CAT ATC GGT ACC ATG GAC CGG GCG-3' (forward), with an introduced Acc65I restriction site, and 5'-TAC CAT ATC GTC GAC TCA GAT GGG TAC-3' (reverse), with an introduced SalI restriction site. PCR reactions contained 8.6 ng of template and 16.5 µg (10 µl, 20 µM) of forward primer and 16.3 µg (10 µl, 20 µM) of reverse primer in a 25 µl volume which was mixed with 25 µl of PCR master mix with a final volume of 50 µl. The thermocycling program used was as follows: pre-denaturation at 95 °C for 5 min then 35 cycles of 95 °C for 1 min, 60 °C for 1 min, and 72 °C for 5 min, and final extension at 72 °C for 10 min. The resulting 4.1 Kb PCR product was then purified using QIAquick columns (Qiagen). The PCR fragment and pQE-30 Xa (Qiagen) were then digested with Acc65I and SalI (New England Biolabs) and the DNA fragments were gel purified using low melt SeaPlaque agarose (Lonza). The DNA bands were visualized using SYBR Safe dye (Invitrogen) and a Dark Reader blue-light transilluminator (Clare Research Inc.) and subsequently excised. The gels slabs were melted at 68 °C and in-gel ligation performed using T4 ligase (New England Biolabs). Ligation reactions HAO PCR product (10 µl, 69 ng), pQE-30 Xa (2.5 µl, 22 ng), ligation buffer (2 µl, 1x final concentration), sterile ddH_2O (4.5 µl), and T4 ligase (1 µl, 400 units) in a final volume of 20 µl. The ligation was performed at room temperature for 1.5 hrs and then placed at

4 °C overnight. The following morning the ligation reaction was removed from the 4 °C and allowed to stand for an addition 1 h at room temperature. The ligation reaction was then melted at 68 °C and diluted to 100 µl with sterile ddH_2O. Then 25 µl of the diluted ligation reaction was transformed into 50 µl of DH5α subcloning efficiency competent cells (Invitrogen). Transformants were plated on LB agar plates containing 100 µg/ml ampicillin and grown overnight at 37 °C. Plasmid DNA from several colonies were isolated using a QIAprep Spin Miniprep Kit (Qiagen) and screened by restriction digestion with Acc65I and SalI. A positive colony was replated and grown over night at 37 °C. Then a single colony was picked and grown up overnight in LB containing 100 µg/ml ampicillin and plasmid DNA isolated using a Wizard II midi prep kit (Promega).

Sequencing of AO containing plasmid- Sequence analysis was performed using a Model 3730 DNA Analyzer from Applied Biosystems (Foster City, CA). The Applied Biosystems BigDye sequencing reaction was used to sequence the DNA. The cDNA(A1717G/K573E mutant) was sequenced in the forward (5') and reverse directions (3') until the forward and reverse data overlapped. This provided the entire sequence for the gene. Individual directions (forward and reverse) were sequenced with overlapping data between analyses. Blast searches were used to compare sequencing data to the known sequence of the gene.

Expression of AO in E.coli- Aldehyde oxidase was overexpressed as an N-terminal 6×His-tag with Factor Xa protease recognition site fusion in TP-1000 cells (a gift from John Enemark's lab). The pQE-30 Xa plasmid containing AO cDNA was transformed into TP-1000 cells and grown on LB agarose plates containing 100 µg/ml ampicillin. A single colony was picked and grown overnight in 100 ml of supplemented LB broth (100 µg/ml ampicillin, 1 µg/ml riboflavin, 50 µM Sodium Molybdate). The overnight culture (10 ml) was used to inoculate 500 ml of supplemented Terrific Broth (100 µg/ml ampicillin, 250 µl of trace element solution containing 2.7g $FeCl_3 \cdot 6H_2O$, 0.2g $ZnCl_2 \cdot 4H_2O$, 0.2g $CoCl_2 \cdot 6H_2O$, 0.2g $Na_2MoO_4 \cdot 2H_2O$, 0.2g $CaCl \cdot 2H_2O$, 0.1g $CuCl_2$, 0.05g H_3BO_3, and 10 ml HCl (conc)

DMD Fast Forward. Published on September 9, 2009 as DOI: 10.1124/dmd.109.029520
This article has not been copyedited and formatted. The final version may differ from this version.

autoclaved in a total volume of 100 ml of di H_2O, 1 µg/ml Riboflavin, plus an additional 50 µM sodium molybdate). Cultures were grown at 37 °C, 250 rpm until an absorbance of 0.4 at 600 nm was reached, 60-90 min, IPTG (1mM) was added for induction and cells were allowed to continue growing at room temperature for 72 hrs at 150 rpm. Cells were harvested by centrifugation at 3500 × g at 4 °C for 30 min. Cell paste was collected and resuspended in equal volumes, 1 g paste to 1 ml of Buffer 1 (100 mM potassium phosphate buffer, 300 mM NaCl, 0.5 µl/ml protease inhibitor cocktail [Sigma P8849]) and frozen at -80 °C.

Mutagenesis- Human AO cDNA in the pQE-30 Xa expression plasmid was mutagenized using the Quikchange II site-directed mutagenesis kit (Stratagene, La Jolla, CA). The mutagenesis was performed using the manufacturer suggested protocol. Primers were designed using the online tool provided by Stratagene. HPLC purified primers were purchased from Invitrogen (Carlsbad, CA). The primers used to generate the wild-type plasmid (E573K) were 5'-aagtaccagaatataggcccaaagcagcatcctgaa-3 (forward) and 5'-ttcaggatgctgctttgggcctatattctggtactt-3' (reverse).

Purification of His tagged AO- Cell suspension was thawed and lysed by adding lysozyme (5 mg/ml), $MgCl_2$ (28.6 µg/ml), RNase (10 µg/ml), DNase (10 µg/ml) and stirring at 4 °C for 60 min. The cell suspension was disrupted by sonication. After centrifugation for 40 min at 100,000g the supernatant was loaded onto a 1 ml HiTrap Chelating HP (Amersham Biosciences, 17-0408-01) charged with Ni^{2+} equilibrated with Buffer 1. The column was washed with 5 ml Buffer 1 and 5 ml of Buffer 2 (100 mM potassium phosphate buffer pH 7.4, 20 mM imidazole, 0.5 µl/ml protease inhibitor cocktail). The HAO was eluted with 3 ml of 100 mM potassium phosphate buffer at pH 7.4, 500 mM imidazole. Protein concentrations were determined by the Bradford assay using bovine serum albumin as a standard and by quantifying flavin adenine dinucleotide content (Massey et al. 1970).

Gel electrophoresis- SDS-PAGE was performed using Phast System (Pharmacia Biotech, Piscataway, NJ) PhastGel Homogeneous 7.5 gels (GE Healthcare, Piscataway, NJ) using the protocol reported in Separation Technique Files No. 111 (Biosciences 1998). Proteins were stained using PhastGel Blue (GE Healthcare) Using development technique File No. 200 (Biosciences 1998).

Tryptic digestion of protein- AO (300 µl, 2.84 µM) was concentrated by trichloroacetic acid precipitation. The protein was resuspended in 8 M urea with 100 mM NH_4HCO_3 follow by addition of DTT to a 5 mM final concentration and incubated at 37 °C for 30 min. Iodoacetamide was then added (1 µl, 25 mM final) and the mixture incubated at 37 °C for an additional 30 min. The solution was diluted to 100 µl with 100 mM NH_4HCO_3 (pH 7.5-8.0) and subsequently digested overnight with trypsin (50 µl, 1 µg) at 37 ºC.

Mass spectrometry- Tryptic digests were analyzed on an Esquire HCT electrospray ion trap mass spectrometer (Bruker Daltonics, Billerica, MA) coupled to a LC Packings Ultimate Nano high-performance liquid chromatography system (instrument). Chromatography was performed with a LC Packings monolithic column using a binary solvent system containing 0.1% formic acid with 3% acetonitrile (solvent A) and 0.1% formic acid with 95% acetonitrile (solvent B) . The sample was eluted using a 5 step linear gradient program of 5% buffer B at 3 min, 15% buffer B at 15 min, 30% buffer B at 60 min, 65% buffer B at 95 min then 100% buffer B at 95.1 min and held at 100% until 115 min with a flow rate of 800 nL/min (Weigert et al. 2008).

Ferricyanide activity assay- Spectrophotometric activity assays using ferricyanide as a single electron acceptor were performed as described by Krenitsky (Krenitsky et al. 1972). The reaction buffer for assays contained 1 mM potassium ferricyanide, 0.13 mM EDTA and 100 mM potassium phosphate buffer (pH 6.8) in a final volume of 1 ml and were incubated at room temperature. Enzyme and substrate concentrations were of adequate concentration to obtain linear initial rates. Substrate concentrations of 6.25, 12.5, 25, 50, 100, 200, and 400 µM were used with 19.12 pmole of AOX1 and 82.15 pmoles of XO.

DMD Fast Forward. Published on September 9, 2009 as DOI: 10.1124/dmd.109.029520
This article has not been copyedited and formatted. The final version may differ from this version.

Reaction progress for the single electron reduction of ferricyanide was monitored by UV at 420 nm and rates were calculated using an extinction coefficient of 2.1 $mM^{-1}cm^{-1}$. The extinction coefficient for the single electron transfer to ferricyanide is 1.040 $mM^{-1}cm^{-1}$, however since the stoichiometry for oxidation of a single substrate is 1 mole to 2 moles of electrons transferred, the extinction coefficient was multiplied by 2. Kinetic parameters were obtained by fitting data to a hyperbola using GraphPad Prism.

Activity assays using quinazolinones and direct UV measurement- Quinazolinone activities were measured using methods similar to those described by Skibo (Skibo et al. 1987). The oxidation of quinazolines was monitored by UV at 270 nm. Assays were performed in buffer containing 100 mM potassium phosphate buffer (pH 7.4), at room tempurature in a final volume of 1 ml. Enzyme and substrate concentrations were of adequate concentration to obtain linear initial rates. For the quinazolinones we used 5 substrates concentrations 12.5, 25, 50, 100, and 200 µM and 118 pmoles of partially purified AOX1. Absorption changes were measured for 2-3 minutes depending on the linearity of the absorption change. Kinetic parameters were obtained by fitting data to a hyperpobola using GraphPad Prism.

Synthesis of quinazolinones- Substituted quinazolinones were synthesized using a microwave-assisted Niementowski reaction (Alexandre et al. 2002). A general procedure is given with the synthesis of compound 1a (Figure 3). Anthranilic acid (200 mg, 1.45 mmol) and formamide (5 ml, reagent-grade) were combined in a 24 mm x 200 mm test tube equipped with ceramic funnel. This tube was irradiated using a standard kitchen microwave oven for a total of 3 min in 1 min intervals with 5 min cooling between irradiation. Prior to the open tube method of preparation, a 15 ml heavy walled pressure tube equipped with a Teflon plug and o-ring was used for the synthesis and the reaction irradiate for 30 min in 5 min intervals with 5 min cooling (preparation of 1c and d Figure 2). **However, we found under these conditions the reaction was prone to explosion.** Thus, we suggest using the open tube method, not the capped tube method. After irradiation and upon cooling, excess formamide was removed by rotary

evaporation and the resulting crude quinazolinones were crystallized from hot ethanol affording a solid. The yields for quinazolinones after crystallization were 41% (1a), 61% (1b), 91% (1c and d) and 34% (1e). The ^{1}H NMR spectra of the products were consistent with literature values. (Orfi et al. 2004; Domarkas et al. 2006) Deuterium exchanges in the C-2 position of 4(3*H*) quinazolinones (1a-e) were accomplished using an uncatalyzed microwave-assisted method (de Keczer et al. 2004). A typical exchange reaction is given with the synthesis of deuterated 1c. To a 15 ml heavy walled pressure tube equipped with a Teflon plug and o-ring were combined 1c (100 mg, 0.684 mmol) with D_2O (2 ml) and CD_3OD (2 ml). The reactions were irradiated using a standard kitchen microwave oven with irradiation times of 2 min (15 sec intervals at 50% power with 2-3 min cooling) and 15 min. Upon cooling, the solvent was removed by rotary evaporation and the reaction repeated until deuterium incorporation was complete as monitored by ^{1}H NMR. Typically three cycles were necessary to achieve deuterium incorporation at the C-2 position of 95% as determined by mass spectral analysis.

Results

The human AO containing vector was constructed by PCR amplifying the protein coding region of AO cDNA from the pCMV6-XL4 plasmid with the addition of flanking Acc65I and SalI restriction sites. The PCR product was then subcloned into a pQE-30 Xa expression vector. The resulting vector construct was sequenced and a single nucleotide mutation found, A1818G (the mutation is A1717G using numbering starting from the start codon of the protein encoding region of the cDNA), translating into a single amino acid mutation, K573E. Comparison of this region in the bovine xanthine oxidase crystal structure (pdb 1V97) shows that this residue is on the exterior of the protein (Okamoto et al. 2004). Site-directed mutagenesis was used to correct this mutation to wild-type and 100% of the coding region is in agreement with the GenBank sequence.

The enzyme was expressed in TP-1000 cells and purified by affinity chromatography. Typically, 20 g of cell paste was obtained from 1 L of growth medium with ~ 5-15 nmol in 1 ml of purified enzyme using our procedures. Figure 2 shows an SDS-PAGE gel of AO before and after purification using a nickel column. The significantly purified protein ran close to the 150 KDa molecular weight marker, and appears to be full length based on this and the tandem MS/MS sequencing.

Purified human AO was reduced, alkylated and subsequently digested with trypsin. The tryptic digest was analyzed by LC-MS/MS. The following tryptic peptides were observed and confirmed by LC-MS/MS: ASELLFYVNGR (4-14), YGCGGGGCGACTVMISR (42-58), HHPANACLIPICSLYGAAVTTVEGIGSTHTR (68-98), FKYPQAPVIMGNTSVGPEVK (257-276), VFFGEGDGIIR (447-457), VFCVGQLVCAVLADSEVQAK (668-687), RVGGAFGGK (802-810), GFGFPQAALITESCITEVAAK (922-942) , FPVGLGSR (1014-1021), GLHGPLTLNSPLTPEK (1295-1310). The observed peptides only account for 12% sequence coverage, but the last peptide covers up to

the last 28 amino acids, while the first covers up to the first 4 amino acids of the 1338 amino acid protein, consistent with full length expression.

We measured the activity of the 6-substituted quinazolinones (Figure 3) in our human AO preparation and the data is given in Table 1. Overall, V/K values increase as the substituents become more electron withdrawing with the exception of R=CH_3. The kinetic isotope effects (KIE) on V/K were determined for substitution of deuterium at the site of oxidation and are given in Table 1. The KIE is significant for all the compounds and increases for the slower reactions.

We repeated these experiments using commercial preparations of bovine xanthine oxidase for comparison with our results for human aldehyde oxidase and the results are shown in Table 2. We chose bovine XO to compare with human AO since it is available commercially, and has been studied extensively. Overall, while the values are not in perfect agreement the trends are similar. The kinetic isotope effects we measured for AO are larger than those of Skibo, however without further study we do not know if this is a significant difference. Uncertainties arise from the fact that the values are not corrected for substrate inhibition, or sulfur incorporation in the cofactor (Schumann et al. 2009) both of which could affect Vmax estimates.

One exception to the general agreement between the kinetic trends in AO and XO is that when we attempted to obtain kinetic parameters for 6-nitroquinazolinone we found that aldehyde oxidase was unable to catalyze this reaction, while under the same conditions we could obtain product with bovine xanthine oxidase. Presently, we are trying to characterize why 6-nitroquinazoinone is not a substrate for AO.

Discussion

Human AOX1 is at present responsible for the metabolism of a number of drugs containing aldehydes and the more prevalent nitrogen heterocycles (Kitamura et al. 2006; Torres et al. 2007). The fraction of drugs metabolized by AOX1 is likely to increase over the next decade. However, the availability of an in vitro system for distinguishing between XO and AOX1 metabolism in humans is lacking. The most commonly used preparation is human liver cytosol, which contain both XO and AOX1. The expression of AOX1 in humans will allow researchers in the field to answer a number of questions that have not been approachable up to this point. Our E. coli expression system should allow for the exploration of the protein structure function relationship by site-directed mutagenesis, and the use of biophysical methods to explore catalysis and binding. Herein, we report the expression and partial purification of AOX1, and use the expressed enzyme to characterize the kinetics of the enzyme without interference from XO.

Human AOX1 cDNA was subcloned into a pQE-30 Xa vector for expression relying on the ground-breaking work of Tanaka and coworkers subcloning of monkey AOX1 (Hoshino et al. 2007). We included a 6X His tag on the amino terminus to aid in purification. No attempt was made to remove the His tag to see if these amino acids alter activity. The resulting plasmid when sequenced was consistent with the 6 X His-wild type AOX1 with a single mutation at A1717G relative to the start codon, translating into a single amino acid mutation, K573E in the expressed protein. Site-directed mutagenesis was used to restore the wild-type sequence.

Expression was achieved in TP1000 E. coli cells (Palmer et al. 1996) using standard expression protocols. The TP1000 E. *coli* strain does not have the mobA and mobB genes that put GMP onto the molybdopterin cofactor. While GMPMoCo is required for binding to E *coli* molybdoenzymes, mammalian enzymes use the GMP-free cofactor. This resulted in between 5 and 15 nmoles of partially purified protein per liter of media based on the flavin optical absorbance at 450 nm. Experiments using cyanide to remove sulfur

from the MoCo in AO resulted in catalytically inactive protein, as expected from previous results with XO (Massey et al. 1970). Obviously, a sulfurase from E. coli is incorporating sulfur into the cofactor, although the specific sulfurase is unknown. Attempts to increase activity, by chemically incorporating sulfur using established protocols were not successful (Wahl and Rajagopalan 1982). Using this procedure we were able to recover cyanide inactivated XO. This lead us to conclude that sulfur incorporation is high in the expressed enzyme although methods for determining the amount of sulfur in the cofactor were not sensitive enough in our hands to determine the sulfur content of the enzyme. One caveat to this conclusion is that we have found the human AO enzyme is not particularly stable to manipulation, and that dialysis for example can inactivate the enzyme.

Purification was accomplished by affinity chromatography using a nickel chelate column, after addition of 6 histidine residues to the amino terminus. The histidine tags did not appear to alter trends in activity and binding affinity, however since this enzyme has never been purified and evaluated some caution is required. Comparison of phthalazine activity (an established AO probe, (Beedham et al. 1990; Obach et al. 2004) in the partially purified enzyme and in human cytosol gave Km values of 29 and 3.7 μM respectively. While this is not a large difference it is outside of the normal 10-15% error we see in determining Km values for AO. This difference could be a result of the histidine affinity tag, or the fact that XO is present in the human cytosol. While to our knowledge, the Km for human XO for phthalazine has not been reported, we measured a 40 μM Km for bovine XO. If human XO has a lower Km it could account for the lower apparent Km in the cytosolic mixture.

We used 6-substituted quinazolinones (Figure 2) to probe the kinetic and chemical mechanism of human AO. We used this series of substrates since previous work by Skibo has established that electron withdrawing groups increase the rates of reaction, and that significant kinetic isotope effects were observed when deuterium replaces hydrogen at the site of oxidation (the 2-position) (Skibo et al. 1987). While it has been speculated that AO and XO have similar mechanisms, almost all mechanistic studies

have been done on XO, and no direct comparison has been made. At present two very similar mechanisms are supported by the literature, both involving nucleophilic attack of a deprotonated water molecule coordinated to the molybdenum with either a concerted hydride transfer, or initial tetrahedral intermediate formation followed by hydride transfer. The results presented in Tables 1 and 2 are consistent with either mechanism with some caveats (Alfaro and Jones 2008),(Doonan et al. 2008), while it requires that the hydride transfer be rate-determining at least to some extent (Schimerlik et al. 1977; Northrop 1981; Ray 1983). The results for AO provide a limited free energy relationship, although for both XO and AOX1 the methyl substituted quinazolinone show very different nonlinear behavior. However, in general electron withdrawing group appear to increase the catalytic efficiency as measured by V/K. The positive slope relative to the Hammett parameters indicates that either a negative charge is developed in the transition state, or that equilibrium addition of the nucleophile increases the concentration of the tetrahedral intermediate increasing the flux of the next step, hydride transfer (Ilich and Hille 1999; Okamoto et al. 2004; Doonan et al. 2005; Hille 2005). To fit the isotope effect data hydride transfer must be rate-limiting, and the trends in kinetic isotope effect support the concerted mechanism (Alfaro and Jones 2008).

The results presented in Tables 1 and 2 also appear to support the conclusion that for substituted quinazolinone substrates the mechanisms for AO and XO are similar but not identical. Two major differences are observed; 1) the 6-nitroquinazolinone is not a substrate for AO, and 2) the kinetic isotope effects appear to be larger for AO than for XO. The contrast between the behavior of the nitro compound in XO, for which it is a very good substrate as reported by Skibo and coworkers (Skibo et al. 1987), and AO which does not turn-over the compound is surprising and unexplained. However, the larger KIE values for AO than XO can be explained in that XO's KIE may be masked by other partially rate-determining steps, while AO hydride transfer is more rate-limiting unmasking the intrinsic KIE value (Northrop 1981; Ray 1983). Studies are ongoing to elaborate on these possible differences in mechanism.

In conclusion, we have expressed human AO in E. coli and have been able to purify protein that is kinetically active. To illustrate the usefulness of this construct we have done a series of kinetic experiments, and compared the kinetic mechanisms of AO and XO, concluding that they share a similar but not identical mechanism. The availability of pure enzyme that can be manipulated by site-directed mutagenesis allows us to compare and contrast human AO with other species. Furthermore, phenotypic variation in human metabolism has not been explored even though over 8 phenotypic variants have been identified (Mwenifumbo and Tyndale 2009). This construct will allow us to understand if any of these variants have functional consequences.

Acknowledgments

We would like to thank Professor John Enemark for sending us TP-1000 E coli cells, Tom Rushmore for providing the human cDNA, and for helpful discussions, and Professor Yorihisa Tanaka for providing monkey AOX which we used to optimize expression conditions.

References

Alexandre, F. R., A. Berecibar and T. Besson (2002). "Microwave-assisted Niementowski reaction. Back to the roots." Tetrahedron Lett. **43**(21): 3911-3913.

Alfaro, J. F. and J. P. Jones (2008). "Studies on the Mechanism of Aldehyde Oxidase and Xanthine Oxidase." J. Org. Chem.

Beedham, C., S. E. Bruce, D. J. Critchley and D. J. Rance (1990). "1-substituted phthalazines as probes of the substrate-binding site of mammalian molybdenum hydroxylases." Biochem. Pharmacol. **39**(7): 1213-21.

Beedham, C., D. J. Critchley and D. J. Rance (1995). "Substrate specificity of human liver aldehyde oxidase toward substituted quinazolines and phthalazines: a comparison with hepatic enzyme from guinea pig, rabbit, and baboon." Arch. Biochem. Biophys. **319**(2): 481-90.

Berger, R., E. Mezey, K. P. Clancy, G. Harta, R. M. Wright, J. E. Repine, R. H. Brown, M. Brownstein and D. Patterson (1995). "Analysis of aldehyde oxidase and xanthine dehydrogenase/oxidase as possible candidate genes for autosomal recessive familial amyotrophic lateral sclerosis." Somat Cell Mol Genet **21**(2): 121-31.

Biosciences, A. (1998). Fast Coomassie staining, Amersham Biosciences UK Limited Amersham Place Little Chalfont Buckinghamshire England HP7 9NA. **200**.

Biosciences, A. (1998). SDS-PAGE in homogeneous media, Amersham Biosciences UK Limited Amersham Place Little Chalfont Buckinghamshire England HP7 9NA. **111**.

de Keczer, S. A., T. S. Lane and M. R. Masjedizadeh (2004). "Uncatalyzed microwave deuterium exchange labeling of bleomycin A(2)." J. Labelled Compd. Radiopharm. **47**(11): 733-740.

Domarkas, J., F. Dudouit, C. Williams, Q. Qiyu, R. Banerjee, F. Brahimi and B. J. Jean-Claude (2006). "The combi-targeting concept: synthesis of stable nitrosoureas designed to inhibit the epidermal growth factor receptor (EGFR)." J. Med. Chem. **49**(12): 3544-52.

Doonan, C. J., N. D. Rubie, K. Peariso, H. H. Harris, S. Z. Knottenbelt, G. N. George, C. G. Young and M. L. Kirk (2008). "Electronic structure description of the cis-MoOS unit in models for molybdenum hydroxylases." J. Am. Chem. Soc. **130**(1): 55-65.

Doonan, C. J., A. Stockert, R. Hille and G. N. George (2005). "Nature of the catalytically labile oxygen at the active site of xanthine oxidase." J. Am. Chem. Soc. **127**(12): 4518-4522.

Dowers, T. S., D. A. Rock, D. A. Rock, B. N. S. Perkins and J. P. Jones (2004). "An analysis of the regioselectivity of aromatic hydroxylation and N-oxygenation by cytochrome P450 enzymes." Drug Metab. Dispos. **32**(3): 328-332.

Garattini, E., M. Fratelli and M. Terao (2008). "Mammalian aldehyde oxidases: genetics, evolution and biochemistry." Cell Mol Life Sci **65**(7-8): 1019-48.

Hille, R. (2005). "Molybdenum-containing hydroxylases." Arch. Biochem. Biophys. **433**(1): 107-116.

Hoshino, K., K. Itoh, A. Masubuchi, M. Adachi, T. Asakawa, N. Watanabe, T. Kosaka and Y. Tanaka (2007). "Cloning, expression, and characterization of male cynomolgus monkey liver aldehyde oxidase." Biol Pharm Bull **30**(7): 1191-8.

Ilich, P. and R. Hille (1999). "Mechanism of formamide hydroxylation catalyzed by a molybdenum-dithiolene complex: A model for xanthine oxidase reactivity." J. Phys. Chem. B **103**(25): 5406-5412.

Kitamura, S., K. Sugihara and S. Ohta (2006). "Drug-metabolizing ability of molybdenum hydroxylases." Drug Metab Pharmacokinet **21**(2): 83-98.

Krenitsky, T. A., S. M. Neil, G. B. Elion and G. H. Hitchings (1972). "A comparison of the specificities of xanthine oxidase and aldehyde oxidase." Arch. Biochem. Biophys. **150**(2): 585-99.

Massey, V., H. Komai, G. Palmer and G. B. Elion (1970). "On the mechanism of inactivation of xanthine oxidase by allopurinol and other pyrazolo[3,4-d]pyrimidines." J Biol Chem **245**(11): 2837-44.

Mendel, R. R. (2007). "Biology of the molybdenum cofactor." J. Exp. Bot. **58**(9): 2289-96.

Moriwaki, Y., T. Yamamoto and K. Higashino (1997). "Distribution and pathophysiologic role of molybdenum-containing enzymes." Histol Histopathol **12**(2): 513-24.

Mwenifumbo, J. C. and R. F. Tyndale (2009). "Molecular genetics of nicotine metabolism." Handb Exp Pharmacol(192): 235-59.

Northrop, D. B. (1981). "Minimal kinetic mechanism and general equation for deuterium isotope effects on enzymic reactions: uncertainty in detecting a rate-limiting step." Biochemistry **20**(14): 4056-61.

O'Brien, S. E. and M. J. de Groot (2005). "Greater than the sum of its parts: combining models for useful ADMET prediction." J. Med. Chem. **48**(4): 1287-91.

Obach, R. S., P. Huynh, M. C. Allen and C. Beedham (2004). "Human liver aldehyde oxidase: inhibition by 239 drugs." J Clin Pharmacol **44**(1): 7-19.

Obach, R. S. and R. L. Walsky (2005). "Drugs that inhibit oxidation reactions catalyzed by aldehyde oxidase do not inhibit the reductive metabolism of ziprasidone to its major metabolite, S-methyldihydroziprasidone: an in vitro study." J Clin Psychopharmacol **25**(6): 605-8.

Okamoto, K., K. Matsumoto, R. Hille, B. T. Eger, E. F. Pai and T. Nishino (2004). "The crystal structure of xanthine oxidoreductase during catalysis: Implications for reaction mechanism and enzyme inhibition." Proc. Natl. Acad. Sci. U. S. A. **101**(21): 7931-7936.

Orfi, L., F. Waczek, J. Pato, I. Varga, B. Hegymegi-Barakonyi, R. A. Houghten and G. Keri (2004). "Improved, high yield synthesis of 3H-quinazolin-4-ones, the key intermediates of recently developed drugs." Curr Med Chem **11**(19): 2549-53.

Palmer, T., C. L. Santini, C. Iobbi-Nivol, D. J. Eaves, D. H. Boxer and G. Giordano (1996). "Involvement of the narJ and mob gene products in distinct steps in the biosynthesis of the molybdoenzyme nitrate reductase in Escherichia coli." Mol. Microbiol. **20**(4): 875-84.

Panoutsopoulos, G. I. and C. Beedham (2004). "Kinetics and specificity of guinea pig liver aldehyde oxidase and bovine milk xanthine oxidase towards substituted benzaldehydes." Acta Biochim. Pol. **51**(3): 649-63.

Rashidi, M. R., J. A. Smith, S. E. Clarke and C. Beedham (1997). "In vitro oxidation of famciclovir and 6-deoxypenciclovir by aldehyde oxidase from human, guinea pig, rabbit, and rat liver." Drug Metab. Dispos. **25**(7): 805-13.

Ray, W. J., Jr. (1983). "Rate-limiting step: a quantitative definition. Application to steady-state enzymic reactions." Biochemistry **22**(20): 4625-37.

Rettie, A. E. and J. P. Jones (2005). "Clinical and toxicological relevance of CYP2C9: Drug-drug interactions and pharmacogenetics." Annual Review of Pharmacology and Toxicology **45**: 477-494.

Schimerlik, M. I., C. E. Grimshaw and W. W. Cleland (1977). "Determination of the rate-limiting steps for malic enzyme by the use of isotope effects and other kinetic studies." Biochemistry **16**(4): 571-6.

Schumann, S., M. Terao, E. Garattini, M. Saggu, F. Lendzian, P. Hildebrandt and S. Leimkuhler (2009). "Site directed mutagenesis of amino acid residues at the active site of mouse aldehyde oxidase AOX1." PLoS One **4**(4): e5348.

Skibo, E. B., J. H. Gilchrist and C. H. Lee (1987). "Electronic probes of the mechanism of substrate oxidation by buttermilk xanthine oxidase: role of the active-site nucleophile in oxidation." Biochemistry **26**(11): 3032-7.

Terao, M., M. Kurosaki, M. M. Barzago, M. Fratelli, R. Bagnati, A. Bastone, C. Giudice, E. Scanziani, A. Mancuso, C. Tiveron and E. Garattini (2009). "Role of the molybdoflavoenzyme aldehyde oxidase homolog 2 in the biosynthesis of retinoic acid: generation and characterization of a knockout mouse." Mol. Cell. Biol. **29**(2): 357-77.

Terao, M., M. Kurosaki, M. M. Barzago, E. Varasano, A. Boldetti, A. Bastone, M. Fratelli and E. Garattini (2006). "Avian and canine aldehyde oxidases - Novel insights into the biology and evolution of molybdo-flavoenzymes." J. Biol. Chem. **281**(28): 19748-19761.

Torres, R. A., K. R. Korzekwa, D. R. McMasters, C. M. Fandozzi and J. P. Jones (2007). "Use of density functional calculations to predict the regioselectivity of drugs and molecules metabolized by aldehyde oxidase." J. Med. Chem. **50**(19): 4642-7.

Wahl, R. C. and K. V. Rajagopalan (1982). "Evidence for the inorganic nature of the cyanolyzable sulfur of molybdenum hydroxylases." J Biol Chem **257**(3): 1354-9.

Weigert, J., M. Neumeier, S. Bauer, W. Mages, A. A. Schnitzbauer, A. Obed, B. Groschl, A. Hartmann, A. Schaffler, C. Aslanidis, J. Scholmerich and C. Buechler (2008). "Small-

interference RNA-mediated knock-down of aldehyde oxidase 1 in 3T3-L1 cells impairs adipogenesis and adiponectin release." FEBS Lett. **582**(19): 2965-72.

Yamaguchi, Y., T. Matsumura, K. Ichida, K. Okamoto and T. Nishino (2007). "Human xanthine oxidase changes its substrate specificity to aldehyde oxidase type upon mutation of amino acid residues in the active site: roles of active site residues in binding and activation of purine substrate." J Biochem **141**(4): 513-24.

Footnotes

Funding for this work was provided by the National Institutes of Health [GM 84546].

Address correspondence to: Jeffrey. P. Jones, Department of Chemistry, Washington State University, Pullman WA 99163. Phone: 505-335-5983, Fax: 509-335-8867, E-mail: jpj@wsu.edu

Legends for figures

Figure 1. Typical oxidations by Xanthine and Aldehyde Oxidases.

Figure 2. SDS PAGE Gel. Lane 1) 10 µl of pre-column lysate. Lane 2) 10 µl of purified Human AO. Lane 3) 10 µl EZ-Run™ Rec Protein Ladder (Fisher BioReagents).

Figure 3. Oxidation of 6-substututed quinazolinones.

Table 1

Kinetic parameters for Human AO metabolism of 6-Substituted Quinazolinones

R=	K_M [a)]	Vmax [b)]	V/K [c)]	KIE [d)]
OCH_3	293	135	461	ND [*]
CH_3	142	22	155	7.6
H	399	240	601	6.3
Cl	27	113	4,185	4.5

[a)] The concentration at half maximal velocity in μM. Errors are around 10% for each value. [b)] The maximum velocity estimated from the asymptote for the hyperbola in nmol/s/mg of enzyme. Errors are around 10% for each value. [c)] V/K multiplied by 1000. [d)] The isotope effect on V/K determined by taking the ratio of V/K for the proton/deuterium substitution at the site of oxidation. [*] ND stands for not determined.

Table 2

Kinetic parameters for Bovine XO metabolism of 6-Substituted Quinazolinones.

R=	K_M [a)]	Vmax [b)]	V/K [c)]	KIE [d)]
OCH_3	85	9	101	ND [*]
CH_3	56	121	2,161	5.2
H	31	17	548	(ND)
Cl	11	164	14,909	3.0

[a)] The concentration at half maximal velocity in μM. Errors are around 10% for each value. [b)] The maximum velocity estimated from the asymptote for the hyperbola in nmol/s/mg of enzyme. Errors are around 10% for each value. [c)] V/K multiplied by 1000. [d)] The isotope effect on V/K determined by taking the ratio of V/K for the proton/deuterium substitution at the site of oxidation from (Skibo et al. 1987). [*] ND stands for not determined.

Figure 1

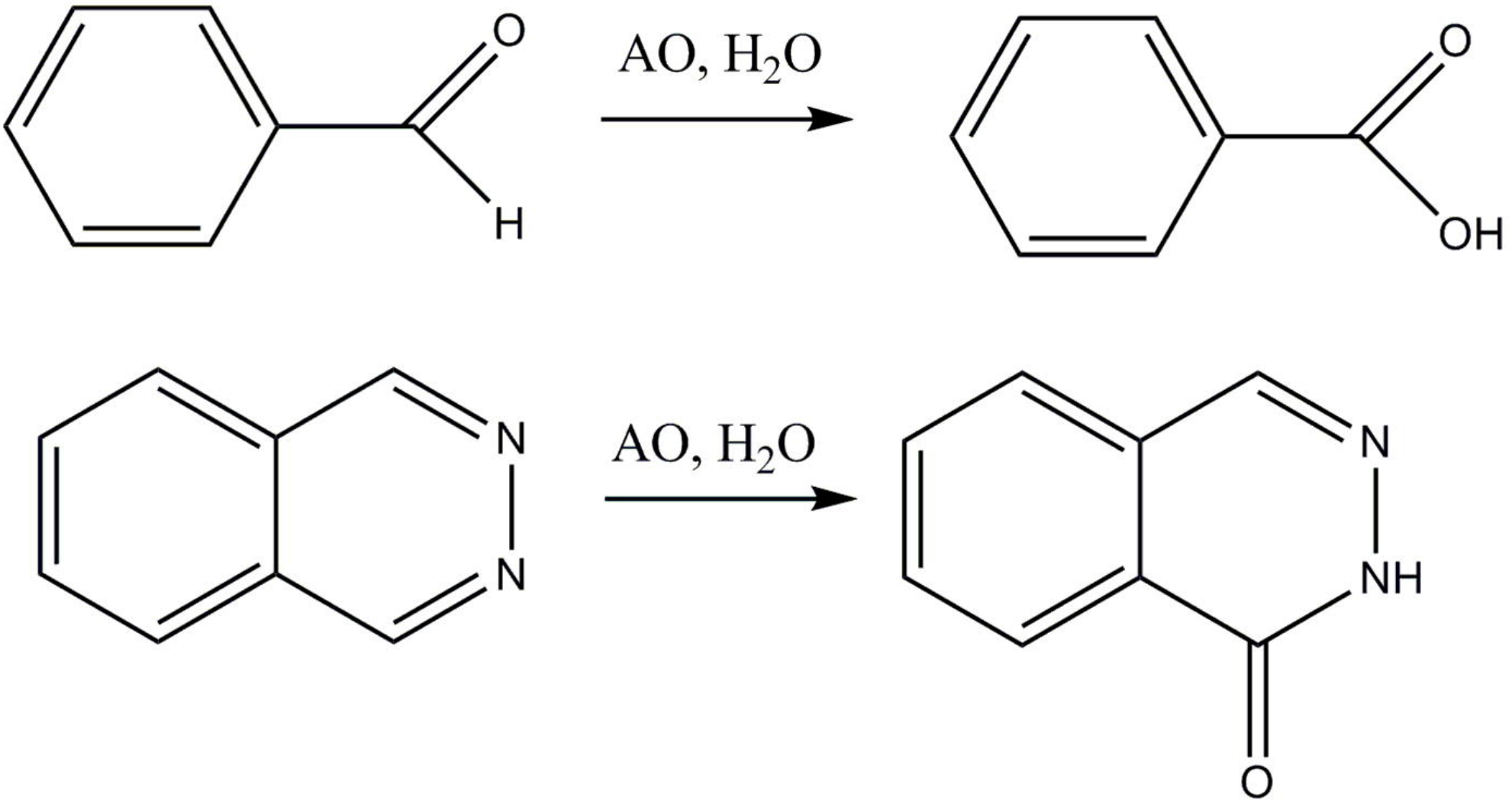

Figure 2

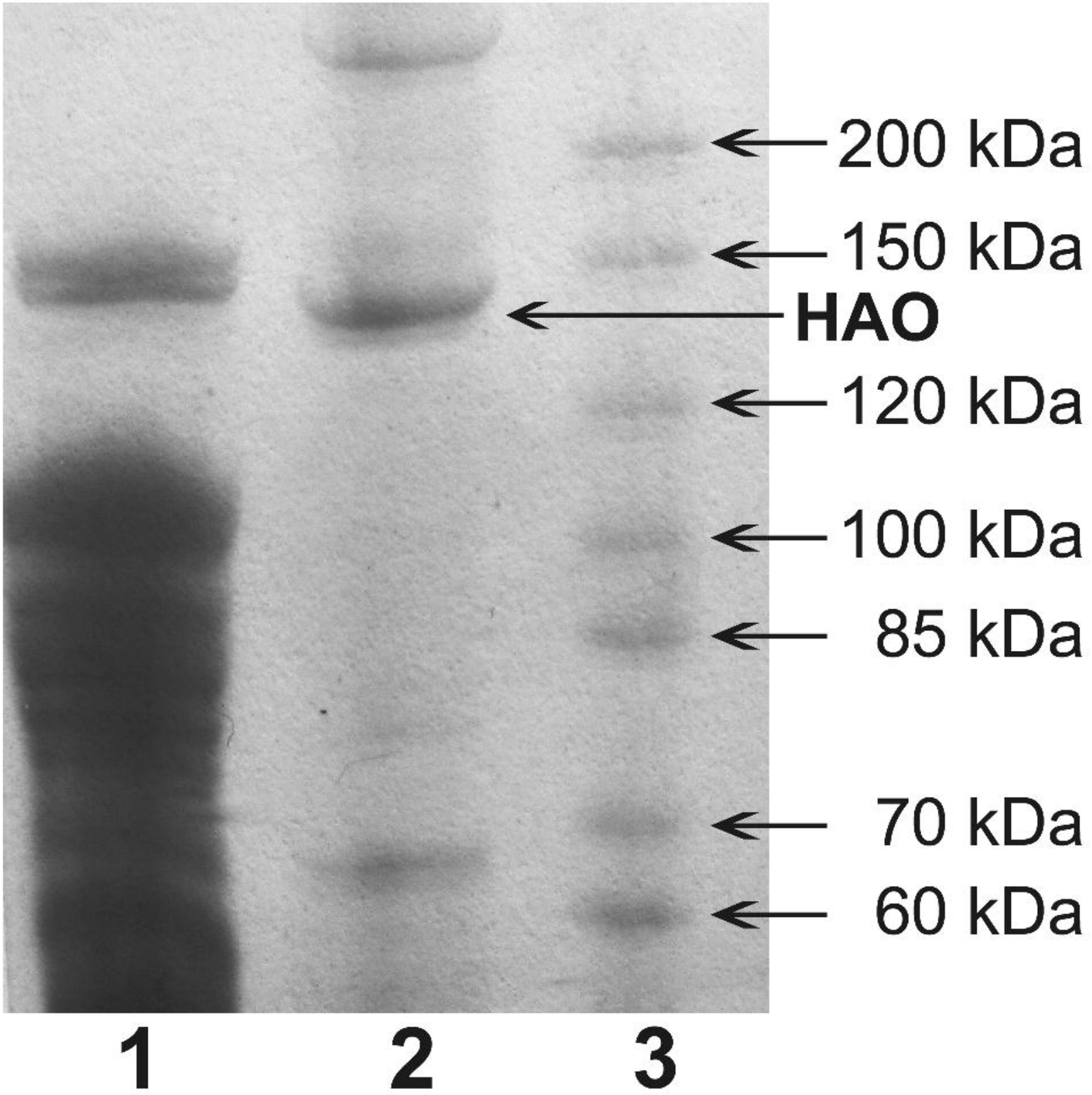

Figure 3

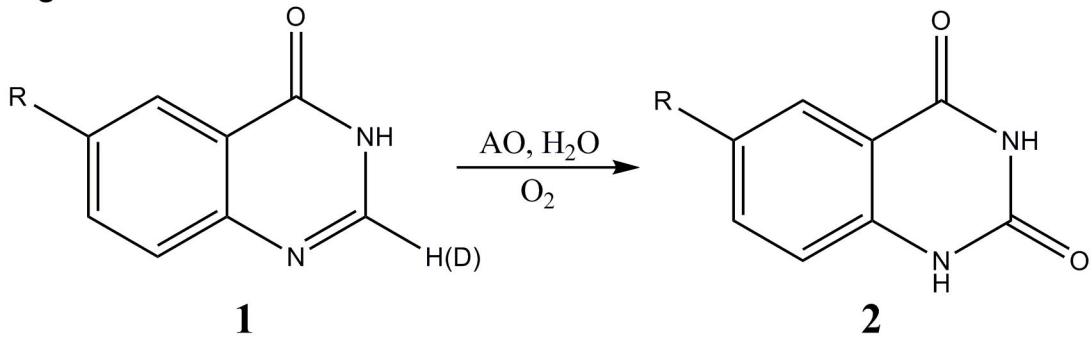

1 **2**

R= OCH_3, a
CH_3, b
H, c
Cl, d
NO_2, e